Bioheat Transfer

Ken, I started with Equation 1, Figure 1, Table 1, Reference 3.

Jonathan W. Valvano

Biomedical Engineering Program

Department of Electrical and Computer Engineering

The University of Texas at Austin

Austin, TX 78712-1084

IV. TISSUE THERMAL TRANSPORT PROPERTIES

A. INTRODUCTION

The transport of thermal energy in living tissue is a complex process involving multiple phenomenological mechanisms including conduction, convection, radiation, metabolism, evaporation, and phase change. The equilibrium thermal properties presented in this chapter were measured after temperature stability had been achieved.

Thermal probe techniques are used frequently to determine the thermal conductivity and the thermal diffusivity of biomaterials [3-6]. Common to these techniques is the use of a thermistor bead either as a heat source or a temperature sensor. Various thermal diffusion probe techniques [7] have been developed from Chato's first practical use of the thermal probe [3]. Physically, for all of these techniques, heat is introduced to the tissue at a specific location and is dissipated by conduction through the tissue and by convection with the blood perfusion.

Thermal probes are constructed by placing a miniature thermistor at the tip of a plastic catheter. The volume of tissue over which the measurement occurs depends on the surface area of the thermistor. Electrical power is delivered simultaneously to spherical thermistor positioned invasively within the tissue of interest. The tissue is assumed to be homogeneous within 1 mL around the probe. The electrical power and the resulting temperature rise are measured by a

microcomputer-based instrument. When the initial tissue temperature is just below the freezing point, the thermistor heat is removed both by conduction and by latent heat. In this situation, the instrument measures effective thermal properties that are the combination of conduction and latent heat. By taking measurements over a range of temperatures, the processes of conduction and latent heat can be separated. When the tissue is perfused by blood, the thermistor heat is removed both by conduction and by heat transfer due to blood flow near the probe. *In vivo*, the instrument measures effective thermal properties that are the combination of conductive and convective heat transfer. Thermal properties are derived from temperature and power measurements using equations that describe heat transfer in the integrated probe/tissue system.

The following five complexities make the determination of thermal properties a technically challenging task. First, tissue heat transfer includes conduction, convection, radiation, metabolism, evaporation, and phase change. It is difficult but necessary to decouple these different heat transfer mechanisms. Second, the mechanical and thermal interactions between the probe and tissue are complex, and must be properly modeled to achieve accurate measurements. When the probe is inserted into living tissue a blood pool may form around the probe because of the mechanical trauma. Because the probe is most sensitive to the tissue closest to it, the presence of a pool of blood will significantly alter the results. Tissue damage due to probe insertion may also occur *in vitro*. Third, the tissue structure is quite heterogeneous within each sample. Thus, the probe (which returns a single measurement value) measures a spatial average of the tissue properties surrounding the active elements. Unfortunately, the spatial average is very nonuniform [8]. The probe is most sensitive to the tissue immediately adjacent to it. It is important to control this effective measurement volume. If the effective volume is too small, then the measurement is highly sensitive to the mechanical/thermal contact between the probe and tissue. If the effective volume is too large, then the measurement is sensitive to the boundary conditions at the surface of the tissue sample. Fourth, there are significant sample to sample and species to species variabilities. One must be careful when extrapolating results obtained in one situation to different situations. Fifth, tissue handling is critical. Thermal properties are

dependent on temperature and water content [9-12]. Blood flow, extracellular water, and local metabolism are factors that strongly affect heat transfer in living tissue, but are difficult to experimentally determine or control. Once a tissue dies, if handled improperly there will be significant water fluxes which will affect tissue thermal properties. Tissues should be stored in a slightly hypertonic saline buffer to minimize tissue mass transfer.

Currently, there is no method to simultaneously quantify the major three parameters: the intrinsic tissue thermal conductivity k_m, the tissue thermal diffusivity α_m, and perfusion w. Either the knowledge of k_m is required prior to the perfusion measurement, or even when k_m is measured in the presence of perfusion, the thermal diffusivity can not be measured [6, 13].

B. BACKGROUND

There are many good reviews of techniques to measure thermal properties [10, 14-16]. Thermophysical Properties of Matter is a ten-volume set that catalogs thermal properties. Volumes 1 and 3 contain thermal conductivity data, and volume 10 contains thermal diffusivity data. Extensive reviews of measurement techniques exist as prefaces to each volume of the set. Additional thermal property data can be found in Eckert and Drake [17]. John Chato has written an excellent chapter in Heat Transfer in Medicine and Biology, edited by Shitzer and Eberhart, which reviews techniques to measure thermal properties of biologic materials [10]. Valvano has documented the temperature dependence of tissue thermal properties [11, 12]. Duck has written an excellent review chapter on this subject [18].

The thermal diffusion probe was conceived by Chato [3, 10]. Significant developments were obtained by Balasubramaniam, Bowman, Chen, Holmes, and Valvano [19-27]. Patel and Walsh have applied the self-heated thermistor technique to non-destructive surface measurements [8, 24-26]. Unfortunately, surface probes are unreliable due to poor probe/tissue contact and uncertain boundary conditions at the tissue surface [8, 24].

Self-heated thermistors have been used to measure perfusion [4, 9, 19, 20, 22-24]. Effective thermal conductivity, k_{eff}, is the total ability of perfused tissue to transfer heat in the

steady state. k_{eff} is the combination of conduction (due to intrinsic thermal conductivity, k_m) and convection (due to perfusion.) Measurements of k_{eff} are very sensitive to perfusion. The limitation of most techniques is that the intrinsic tissue thermal conductivity must be known in order to accurately measure perfusion. Holmes and Chen use a combination of steady state and transient heating modes to determine perfusion without requiring a no flow calibration measurement [13, 19, 20]. The uncertainty of k_m significantly limits the perfusion accuracy [9].

C. MEASUREMENT OF THERMAL CONDUCTIVITY AND DIFFUSIVITY

1. Methods

In the constant temperature heating technique, the instrument first measures the baseline tissue temperature, T_0. Then, an electronic feedback circuit applies a variable voltage, V(t), in order to maintain the average thermistor temperature at a predefined constant, T_h. The applied thermistor power includes a steady state and a transient term:

$$P(t) = A + Bt^{-1/2} \qquad (1)$$

In order to measure thermal conductivity, thermal diffusivity, and tissue perfusion the relationship between applied thermistor power, P, and resulting thermistor temperature rise, $\Delta T(t)=T_h-T_0$, must be known. In the constant temperature method, the ΔT is constant. The thermistor bead is treated as a sphere of radius ‘a’ embedded in a homogeneous medium. Since all media are considered to have constant parameters with respect to time and space, the initial temperature will be uniform when no power is supplied to the probe.

$$T_b = T_m = T_0 = T_a + \frac{Q_{met}}{wc_{bl}} \quad \text{at} \quad t = 0 \qquad (2)$$

Let V be the temperature rise above baseline, $V=T-T_0$. Both the thermistor bead temperature rise (V_b) and the tissue temperature rise (V_m) are initially zero.

$$V_b = V_m = 0 \qquad \text{at} \quad t = 0 \qquad (3)$$

Assuming the venous blood temperature equilibrates with the tissue temperature and that the metabolic heat is uniform in time and space, the Pennes' bioheat transfer equation in spherical coordinates is given by [28].

$$\rho_b c_b \frac{\partial V_b}{\partial t} = k_b \frac{1}{r^2} \frac{\partial}{\partial r}\left(r^2 \frac{\partial V_b}{\partial r}\right) + \frac{A+Bt^{-1/2}}{\frac{4}{3}\pi a^3} \qquad r < a \qquad (4)$$

$$\rho_m c_m \frac{\partial V_m}{\partial t} = k_m \frac{1}{r^2} \frac{\partial}{\partial r}\left(r^2 \frac{\partial V_m}{\partial r}\right) - w c_{bl} V_m \qquad r > a \qquad (5)$$

Perfect thermal contact is assumed between the finite-sized spherical thermistor and the infinite homogeneous perfused tissue. At the interface between the bead and the tissue, continuity of thermal flux and temperature leads to the following boundary conditions:

$$V_b = V_m \qquad \text{at } r = a \qquad (6)$$

$$k_b \frac{\partial V_b}{\partial r} = k_m \frac{\partial V_m}{\partial r} \qquad \text{at } r = a \qquad (7)$$

The other boundary conditions are necessary at positions $r \rightarrow 0$ and $r \rightarrow \infty$. Since no heat is gained or lost at the center of the thermistor:

$$V_b = \text{finite} \left(\text{or } k_b \frac{\partial V_b}{\partial r} = 0 \right) \qquad \text{as } r \rightarrow 0 \qquad (8)$$

Because the thermistor power is finite and the tissue is infinite, the tissue temperature rise at infinity goes to zero:

$$V_m \rightarrow 0 \qquad \text{as } r \rightarrow \infty \qquad (9)$$

It is this last initial condition that allows the Laplace transform to be used to solve the coupled partial differential equations. The Laplace transform converts the partial differential equations into ordinary differential equations that are independent of time t. The steady state solution allows for the determination of thermal conductivity and perfusion [20].

$$V_b(r) = \frac{A}{4\pi a\, k_b}\left[\frac{k_b}{k_m(1+\sqrt{z})} + \frac{1}{2}\left(1 - \left(\frac{a}{r}\right)^2\right)\right] \qquad (10)$$

$$V_m(r) = \frac{A}{4\pi r\, k_m}\left[\frac{e^{(1-r/a)\sqrt{z}}}{1+\sqrt{z}}\right] \qquad (11)$$

where z is a dimensionless Pennes' model perfusion term ($wc_{bl}a^2/k_m$). The measured thermistor response, ΔT, is assumed be the simple volume average of the thermistor temperature:

$$\Delta T = \frac{\int_0^a V_b(r)\, 4\pi r^2\, dr}{\frac{4}{3}\pi a^3} \qquad (12)$$

Inserting Eq. (10) into Eg. (12) yields the relationship used to measure thermal conductivity assuming no perfusion [4].

$$k_m = \frac{1}{\frac{4\pi a \Delta T}{A} - \frac{0.2}{k_b}} \qquad (13)$$

A similar equation allows the measurement of thermal diffusivity from the transient response, again assuming no perfusion [22].

$$\alpha_m = \left[\frac{a}{\sqrt{\pi}\, B/A \;(1 + 0.2 \frac{k_m}{k_b})} \right]^2 \qquad (14)$$

Rather than using the actual probe radius (a) and probe thermal conductivity (k_b), the following empirical equations are used to calculate thermal properties.

$$k_m = \frac{1}{\frac{c_1 \Delta T}{A} + c_2} \qquad (15)$$

$$\alpha_m = \left[\frac{c_3}{\sqrt{\pi}\, B/A \;(1 + 0.2 \frac{k_m}{c_4})} \right]^2 \qquad (16)$$

The coefficients c_1, c_2, c_3, and c_4 are determined by operating the probe in two materials of known thermal properties. Typically agar-gelled water and glycerol are used as thermal standards. This empirical calibration is performed at the same temperatures at which the thermal property measurements will be performed.

It is assumed that the baseline tissue temperature, T_0, is constant during the 30-second transient. Patel has shown that if the temperature drift, dT_0/dt, is larger than 0.1 ˚C/min, then significant errors will occur [8]. The electronic feedback circuit forces T_h to a constant. Thus, if T_0 is constant then ΔT does not vary during the 30-second transient.

The applied power, P(t), varies during the 30 second transient. Linear regression is used to calculate the steady state and transient terms in Eq. (1). Figure 1 shows some typical responses. The steady state response (time equals infinity) is a measure of the thermal conductivity. The transient response (slope) indicated the thermal diffusivity.

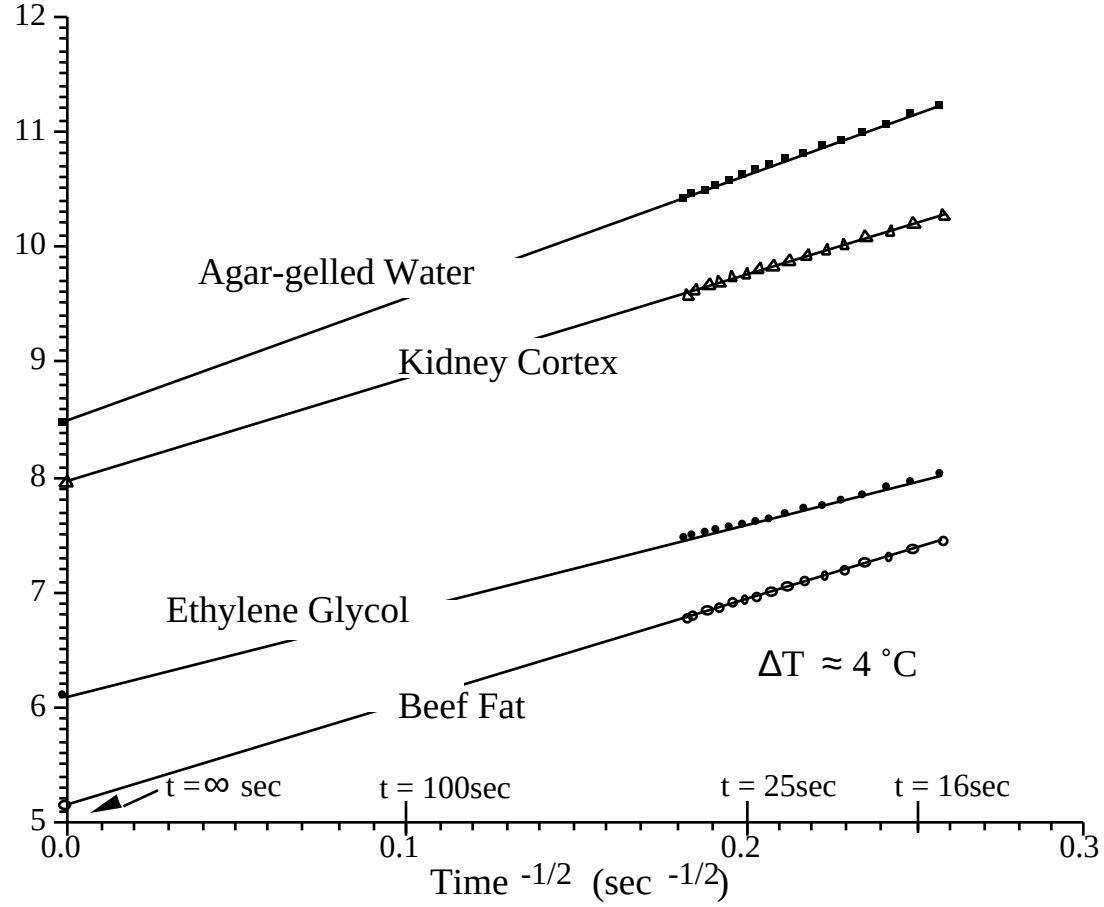

Figure 1. Typical P/ΔT versus time$^{-1/2}$ data for the constant temperature heating technique.

The time of heating can vary from 10 to 60 seconds. Shorter heating times are better for small tissue samples and for situations where there is baseline tissue temperature drift. Another advantage of shorter heating times is the reduction in the total time required to make one measurement. Longer heating times increase the measurement volume and reduce the effect of imperfect thermistor/tissue coupling. Typically, shorter heating times are used *in vivo* because it

allows more measurements to be taken over the same time period. On the other hand, longer heating times are used *in vitro* because accuracy is more important than measurement speed.

2. Probe design

Thermal probes must be constructed in order to measure thermal properties. The two important factors for the thermal probe are thermal contact and transducer sensitivity. The shape of the probe should be chosen in order to minimize trauma during insertion. Any boundary layer between the thermistor and the tissue of interest will cause a significant measurement error. The second factor is transducer sensitivity that is the slope of the thermistor voltage versus tissue thermal conductivity. Equation (13) shows for a fixed ΔT k_m and k_b the thermistor power (A) increases linearly with probe size (a). Therefore larger probes are more sensitive to thermal conductivity. Thermometrics P60DA102M and Fenwal 121-102EAJ-Q01 are glass probe thermistors that make excellent transducers. The glass coated spherical probes provide a large bead size and a rugged, stable transducer. The Thermometrics BR55KA102M and Fenwal 112-102EAJ-B01 bead thermistors also provide excellent results. For large tissue samples multiple thermistors can wired in parallel, so they act electrically and thermally as one large device. There are two advantages to using multiple thermistors. The effective radius, $a=c_1/4\pi$, is increased from about 0.1 cm for a typical single P60DA102M probe to about 0.5 cm for a configuration of three P60DA102M thermistors. The second advantage is that the three thermistors are close enough to each other that the tissue between the probes will be heated by all three thermistors. This cooperative heating tends to increase the effective measurement volume and reduce the probe/tissue contact error. Good mechanical/thermal contact is critical. The probes are calibrated after they are constructed, so that the thermistor geometry is incorporated into the coefficients c_1, c_2, c_3, and c_4. The same water bath, and probe configuration should be used during the calibration and during the tissue measurements.

3. Calibration

Calibration is a critical factor when using an empirical technique. For temperatures below 0 ˚C, ice and ethylene glycol are used as thermal standards. For temperatures between 0 and 15 ˚C, agar-gelled water and ethylene glycol can be used as thermal standards. For temperatures between 15 and 75 ˚C, agar-gelled water and glycerol were used. One gram of agar per 100 mL of water should be added to prevent convection. The instrument has been used to measure k_m and α_m of various concentrations of agar-gelled water at 37˚C.

A mixture of water and glycerol can be used to estimate the accuracy of the technique. The mass fraction, m, can be used to determine the true thermal properties of the mixture [29].

$$k_m = m\,k_g + (1-m)k_w + 1.4\,m\,(m-1)(k_w - k_g - 2) - 0.014\,m\,(m-1)(T - 20^{\circ}C) \quad (17)$$

$$\alpha_m = m\,\alpha_g + (1-m)\,\alpha_w \quad (18)$$

D. ESTIMATION OF HEAT TRANSFER COEFFICIENT

1. Introduction

The topologies of the inner surfaces of the heart and blood vessels are very complex. Consequently, it is very difficult to model the heat transfer at the wall analytically. Any attempt to estimate the heat transfer coefficient analytically will be inaccurate because of the complex contours of structures like the endocardium. The experimental method presented in this section to estimate the heat transfer coefficient, hence, is very appropriate.

The following method can be used to estimate the convective coefficient due to the blood flow inside the chambers of the heart. This method can be also applied to blood vessels as well. The method to measure the convective coefficient due to blood flow inside the heart is derived from basic heat transfer analysis. Two miniature thermistor (BR11, Thermometrics Inc.) probes

are inserted at fixed locations near the inner surface of the model. T_1 is the measured temperature nearest the endocardial wall, and T_2 is measured 2 mm inside the myocardial wall. The epicardial surface of the heart is maintained at a steady temperature, T_o. Blood at a different temperature T_b is pumped through the heart. The thermistor probes are used to continuously monitor the spatial temperature gradient in the heart muscle. The basic principle used to estimate the heat transfer coefficient, *h*, is as follows:

$$h\ (T_{blood} - T_1) = k_s \left.\frac{dT}{dn}\right|_{blood}, \qquad (19)$$

where n is the direction perpendicular to the surface. k_s is the thermal conductivity of the heart wall. The gradient at the wall of the surface is calculated from the data obtained from the array of thermistors.

2 Calibration

Ideally the temperature measured in any experiment should be the temperature of the zero-volume point of interest. But when a measurement is made the temperature sensor has a finite volume and the actual measurement is the volume-averaged measurement of some region around the sensor. Similarly the gradient measured using two sensors is an estimate of the gradient between the two sensors. These two errors are responsible for the estimate of the heat transfer coefficient measured using the Eq. (19) to be vastly different from the correct value. Hence the probe assemble is first calibrated by operating the probe in situations where the true convective heat transfer coefficient is known. Two calibration factors, c_1 c_2, are added to Eq.

(19) to adjust for the finite size of the temperature sensors, and for the fact the that the measured temperature gradient is not at the wall surface.

$$h = c_1 \exp\left(c_2 \frac{k_s (T_1 - T_2)}{(T_f - T_1)}\right) \qquad (20)$$

where T_1 and T_2 are measured temperatures in the wall. A cylindrical tube made with a material (e.g., silicone) that has thermal properties close to tissue can be used to calibrate the sensor-combination. The key to accurate measurements lies in how close the calibration configuration matches the actual experimental conditions.

3 Verification

The effect of the measurement errors on the estimate of the heat transfer coefficient was studied for a tube of inner radius R_i (0.73 cm) and outer radius of R_o (1.33 cm). The temperature distribution inside the tube wall was analytically determined for water following inside and with the outer wall temperature held at a constant temperature of 23 ˚C. The heat transfer coefficient was then calculated from the temperature distribution using the relation in Eq. (19). The effect of the measurement errors on the heat transfer coefficient estimate was analyzed by using values for the temperature and the gradient away from the wall of the tube.

The temperature at any point at distance of R from the axis of the tube is given by

$$T = T_o - B_i (T_i - T_w) \ln\left(\frac{R}{R_o}\right), \qquad (21)$$

where, the T_w is the inner wall temperature given by

$$T_w = \frac{T_o - B_i \ln\left(\frac{R_i}{R_o}\right) T_i}{1 - B_i \ln\left(\frac{R_i}{R_o}\right)} \qquad (22)$$

where, T_o is the Outer wall temperature, Bi is the Biot number calculated as (hR_i/k), and h is the heat transfer coefficient and k is the thermal conductivity of the material of the tube.

4. *In Vitro* Studies

The first *in vitro* study used two cylindrical tubes. The first tube was used to calibrate the probe and the second to evaluate measurement accuracy. The exact position of placement of the thermistor array for sensing the temperature must be in a similar location relative to the inner wall for both the calibration and measurement. The water at 37 ^oC was made to flow through the tube at a rate of L (L/min). The flow was measured using a rotometer type flowmeter (accuracy 2%, Omega Engineering Inc.). The temperature gradients were recorded continuously.

The tube was initially maintained at the room temperature. The water at 37 ^oC was made to flow through the tube. For a smooth tube of cylindrical cross section the relation between Nu, Re and Pr, for turbulent flow conditions, is given by,

$$Nu_D = \frac{(f/8)(Re_D - 1000)Pr}{1 + 12.7(f/8)^{1/2}(Pr^{2/3} - 1)}, \quad (23)$$

where the friction factor, f is

$$f = (0.790 \ln Re_D - 1.64)^{-2} \quad (24)$$

This correlation is valid for $0.5 < Pr < 2000$ and $2300 < Re_D < 5 \times 10^6$. The setup was calibrated with a tube of 1.46 cm diameter and then tested with a tube of 1.27 cm. The flow rates were selected to give a range of h values from 800 to 4000 watts/m^2-K. The average accuracy is about 10%.

E. TEMPERATURE DEPENDENT THERMAL PROPERTIES

1. Temperature Dependence of Organ Tissue

When modeling heat transfer in situations where the temperature range exceeds 10 ˚C it is important to consider the temperature dependence of the tissue thermal properties. Valvano measured tissue thermal properties as a function of temperature using the constant ΔT thermistor heating technique [11, 12]. The results shown in Table 1 were derived from *in vitro* measurements taken at 3, 10 17, 23, 30, 37, and 45 ˚C.

Tissue	Species	k_0 mW/cm˚C	k_1 mW/cm˚C^2	α_0 cm^2/sec	α_1 cm^2/sec˚C
Adenocarinoma of the Breast	Human	4.194	0.03911	0.001617	-0.000049
Cerebral Cortex	Human	5.043	0.00296	0.001283	0.000050
Colon Cancer	Human	5.450	(at 19˚C)	0.001349	(at 19˚C)
Fat of Spleen	Human	3.431	-0.00254	0.001321	-0.000002
Liver	Human	4.692	0.01161	0.001279	0.000036
Liver	Pig	4.981	0.00800	0.001240	0.000053
Liver	Rabbit	4.668	0.02601	0.001370	0.000178
Lung	Human	3.080	0.02395	0.001071	0.000082
Lung	Human	4.071	0.01176	0.001192	0.000031
Lung	Pig	2.339	0.02216	0.000695	0.000080
Myocardium	Dog	4.869	0.01332	0.001296	0.000058
Myocardium	Human	4.925	0.01195	0.001289	0.000050
Myocardium	Pig	4.841	0.01333	0.001270	0.000051
Pancreas	Dog	4.790	0.00849	0.001287	0.000062
Pancreas	Human	4.365	0.02844	0.001391	0.000084
Pancreas	Pig	4.700	0.00194	0.001530	0.000130
Renal Cortex	Dog	4.905	0.01280	0.001333	0.000039
Renal Cortex	Human	4.989	0.01288	0.001266	0.000055
Renal Cortex	Pig	4.967	0.01176	0.001284	0.000039
Renal Cortex	Rabbit	4.945	0.01345	0.001311	0.000027
Renal Medulla	Dog	5.065	0.01298	0.001305	0.000063
Renal Medulla	Human	4.994	0.01102	0.001278	0.000055
Renal Pelvis	Dog	4.930	0.01055	0.001334	0.000052
Renal Pelvis	Human	4.795	0.01923	0.001329	0.000011
Spleen	Human	4.913	0.01300	0.001270	0.000047
Spleen	Rabbit	4.863	0.01267	0.001257	0.000042

Table 1. Thermal properties as a function of temperature [9].

The animal tissues were measured from freshly sacrificed dogs, rabbits, and pigs. The normal human tissues were obtained from autopsy. The human cancers were freshly excised. The k_0, k_1, α_0, and α_1 values are the linear fit of the thermal properties as a function of temperature.

$$k = k_0 + k_1 T \quad (25)$$

$$\alpha = \alpha_0 + \alpha_1 T \quad (26)$$

The average thermal properties of this data are

$$k = 4.574 + 0.01403 T \quad (27)$$

$$\alpha = 0.001284 + 0.000053 T \quad (28)$$

where conductivity is in mW/cm˚C, diffusivity is in cm^2/sec and temperature is in ˚C.

2. Temperature Dependence of Human Arterial Tissue

Aortic tissue was obtained from a local pathology lab. The thermal probes were placed on the endothelial surface of the aortic wall, and the tissue/probe combination was wrapped in plastic. The tissue surface was kept wet to improve the thermal contact and to prevent drying. The samples were placed in a breaker of saline and the breaker was put into a temperature controlled water bath. Thermal conductivity and thermal diffusivity were measured ten times at each temperature 35, 55, 75, and 90˚C. The measurement order was varied between 35,55,75,90 95,75,55,35 75,90,55,35 and 55,35,90,75. Measurements were obtained from both normal and diseased tissue. The plaques were categorized by gross visual observation. The calcified plaques were hard and bony. The fibrous plaques were firm but pliable. The fatty plaques were loose and buttery. The results from 54 tissues are presented in Tables 2 and 3. The column n refers to the number of tissue samples. The standard deviation is given in the parentheses.

Tissue	n	at 35˚C	at 55˚C	at 75˚C	at 90˚C
Normal aorta	12	4.76 (0.41)	5.03 (0.60)	5.59 (0.37)	6.12 (0.12)
Fatty plaque	13	4.84 (0.44)	4.97 (0.49)	5.46 (0.54)	5.88 (0.81)
Fibrous plaque	12	4.85 (0.22)	5.07 (0.30)	5.38 (0.38)	5.77 (0.56)
Calcified plaque	17	5.02 (0.59)	5.26 (0.73)	5.81 (0.82)	6.19 (0.85)

Table 2. Thermal conductivity (mW/cm-˚C) of human aorta and atherosclerotic plaque [12].

Tissue	n	at 35˚C	at 55˚C	at 75˚C	at 90˚C
Normal aorta	12	1.27 (0.07)	1.33 (0.11)	1.44 (0.10)	1.56 (0.05)
Fatty plaque	13	1.28 (0.05)	1.32 (0.06)	1.41 (0.11)	1.46 (0.15)
Fibrous plaque	12	1.29 (0.03)	1.36 (0.07)	1.41 (0.10)	1.52 (0.20)
Calcified plaque	17	1.32 (0.07)	1.37 (0.12)	1.53 (0.17)	1.66 (0.20)

Table 3. Thermal diffusivity (*1000 cm^2/sec) of human aorta and atherosclerotic plaque [12].

The two sample t-test with p=0.05 was used to determine significant differences. The tissue thermal properties increased with temperature and were significantly less than water. The measurement order did not affect the measured thermal properties. There was no difference between the thermal conductivity of normal aorta, fatty plaque and fibrous plaque. The thermal conductivity and thermal diffusivity of calcified plaque were slightly higher than normal aorta, fatty plaque and fibrous plaque.

3. Temperature Dependence of Canine Arterial Tissue

Carotid and femoral arteries were harvested immediately *post mortem*. The thermal probes were placed on the endothelial surface of the arterial wall. Thermal conductivity and thermal diffusivity were measured ten times at each temperature 25, 35, 45, 55, 65, 75, 85, and 95˚C. Measurements were obtained only from normal tissue. The results from 18 tissues are summarized in Eqs. (29)-(33).

Canine femoral artery

$$k\ (mW/cm\text{-}^\circ C) = 3.688 + 0.0062014\ T\ (^\circ C) \quad (29)$$

$$\alpha\ (cm^2/sec) = 0.001003 + 0.000001381\ T\ (^\circ C) \quad (30)$$

Canine carotid artery

$$k\ (mW/cm\text{-}^\circ C) = 4.480 + 0.0000164\ T\ (^\circ C) \quad (31)$$

$$\alpha\ (cm^2/sec) = 0.001159 + 0.000003896\ T\ (^\circ C) \quad (32)$$

The two sample t-test with p=0.01 shows that both thermal conductivity and thermal diffusivity are larger in carotid versus femoral artery. These results could be explained from the fact that the carotid artery contains more collagen than femoral artery. A tissue with a higher percentage of collagen would have lower thermal properties because collagen is a thermal insulator.

4. Temperature Dependence of Swine Left Ventricle

Swine myocardial samples were harvested immediately *post mortem*. The thermal probes were placed on the left ventricular muscle. Thermal conductivity and thermal diffusivity were measured ten times at each temperature 25, 37. 50, 62 and 76˚C. Measurements were obtained only from normal tissue. The results are summarized in Tables 4 and 5.

Temperature	25 ˚C	37 ˚C	50 ˚C	62 ˚C	76 ˚C
	5.23	5.14	5.17	4.39	5.24
	5.07	5.12	4.75	3.30	4.29
	5.30	5.21	5.61	5.67	4.83
	5.43	5.54	4.22	4.16	5.89
	4.68	5.35	4.93	5.33	5.23
	5.25	5.08	4.84	5.70	5.39
	5.27	5.48	4.42	5.11	4.75
	5.28	4.57	4.93	4.99	3.25
	5.86	5.76	5.52	5.03	2.69
	4.78	5.10	5.88	5.30	5.28
	4.75	5.35	5.35	4.67	5.60
	4.92	6.02	5.60	5.49	4.68
Mean	5.15	5.31	5.1	4.93	4.76
Std. Dev.	0.33	0.37	0.51	0.70	0.95

Table 4. Thermal Conductivity ($mW \cdot cm^{-1} \cdot K^{-1}$) of Myocardial Tissue

Temperature	25 ˚C	37 ˚C	50 ˚C	62 ˚C	76 ˚C
	0.00151	0.00170	0.00165	0.00159	0.00167
	0.00154	0.00147	0.00203	0.00235	0.00249
	0.00143	0.00165	0.00151	0.00169	0.00166
	0.00146	0.00143	0.00116	0.00191	0.00229
	0.00159	0.00160	0.00176	0.00167	0.00173
	0.00141	0.00178	0.00179	0.00163	0.00185

	0.00165	0.00149	0.00235	0.00143	0.00185
	0.00132	0.00206	0.00179	0.00170	0.00199
	0.00141	0.00144	0.00147	0.00143	0.00062
	0.00168	0.00179	0.00160	0.00180	0.00167
	0.00154	0.00156	0.00173	0.00161	0.00173
	0.00164	0.00138	0.00171	0.00169	0.00192
Mean	0.00152	0.00161	0.00171	0.00171	0.00179
Std. Dev.	0.00012	0.00020	0.00031	0.00025	0.00047

Table 5. Thermal Diffusivity ($cm^2 \cdot s^{-1}$) of Myocardial Tissue

5. Thermal Properties of Frozen Tissue

The thermal properties of frozen tissue are significantly different from normal tissue. Valvano measured frozen tissue thermal properties using the constant ΔT thermistor heating technique [30]. The results shown in Table 6 were derived from *in vitro* measurements taken at -18, -5, and +0.1 ˚C.

T (˚C)	N	M	Species Tissue	k_m(mW/cm˚C)	α_m(1000*cm^2/sec)
+0.1	45	6	Bovine Kidney Cortex	4.54 (±0.16)	1.18 (±0.09)
-5	15	4	Bovine Kidney Cortex	15.35 (±1.09)	4.71 (±0.99)
-18	18	3	Bovine Kidney Cortex	13.72 (±0.73)	6.84 (±0.83)
+0.1	66	9	Bovine Liver	4.17 (±0.13)	1.05 (±0.09)
-5	66	9	Bovine Liver	13.96 (±2.49)	4.77 (±0.58)
-18	56	8	Bovine Liver	9.89 (±0.44)	5.71 (±0.74)
+0.1	48	6	Bovine Muscle	4.25 (±0.37)	1.05 (±0.11)
-5	42	7	Bovine Muscle	13.93 (±1.23)	5.37 (±0.97)
-18	60	8	Bovine Muscle	10.76 (±1.14)	6.84 (±1.10)
+0.1	21	3	Bovine Fat	1.93 (±0.12)	0.59 (±0.13)
-5	32	4	Bovine Fat	2.66 (±0.38)	0.98 (±0.19)
-18	24	4	Bovine Fat	2.80 (±0.53)	1.54 (±0.57)

Table 6. Average thermal properties. N is the number of measurements and M is the number of tissues. (±0.xx) is the standard deviation of the average [30].

5. Thermal Properties As A Function Of Water And Fat Content

In a global sense, the thermal properties of tissue are determined by the relative concentrations of its constituate parts. Spells found a linear relationship between tissue thermal conductivity and water content [31]:

$$k\ (mW/cm\text{-}^{\circ}C) = 0.54 + 5.73\ m_{water} \text{ for } m_{water}>0.2 \qquad (33)$$

where m_{water} is the mass fraction of water in the tissue. Cooper and Trezek found an empirical relationship between thermal conductivity and mass fractions of water, protein and fat [32].

$$k\ (mW/cm\text{-}^{\circ}C) = \rho \sum_{n} \frac{k_n\ m_n}{\rho_n} = \rho\ (6.28\ m_{water} + 1.17\ m_{protein} + 2.31\ m_{fat}) \qquad (34)$$

Cooper and Trezek [32] found similar relationships for specific heat and density.

$$c\ (J/g\text{-}^{\circ}C) = \sum_{n} c_n\ m_n = 4.2\ m_{water} + 1.09\ m_{protein} + 2.3\ m_{fat} \qquad (35)$$

$$\rho\ (g/cm^3) = \frac{1}{\sum_{n} \frac{m_n}{\rho_n}} = \frac{1}{m_{water} + 0.649\ m_{protein} + 1.227\ m_{fat}} \qquad (36)$$

IV. EFFECT OF BLOOD FLOW ON TEMPERATURE

A. INTRODUCTION

Bioheat transfer processes in living tissues are often influenced by the influence of blood perfusion through the vascular network on the local temperature distribution. When there is a significant difference between the temperature of blood and the tissue through which it flows,

convective heat transport will occur, altering the temperatures of both the blood and the tissue. Perfusion based heat transfer interaction is critical to a number of physiological processes such as thermoregulation and inflammation.

The blood/tissue thermal interaction is a function of several parameters including the rate of perfusion and the vascular anatomy, which vary widely among the different tissues, organs of the body, and pathology. Appendix B contains an extensive compilation of perfusion rate data for many tissues and organs and for many species. The literature on mathematical modeling of the influence of blood perfusion on bioheat transfer phenomena has been reviewed recently by Charney [33], and this reference is highly recommended for readers desiring an in-depth presentation of the topic.

The rate of perfusion of blood through different tissues and organs varies over the time course of a normal day's activities, depending on factors such as physical activity, physiological stimulus and environmental conditions. Further, many disease processes are characterized by alterations in blood perfusion, and some therapeutic interventions result in either an increase or decrease in blood flow in a target tissue. For these reasons, it is very useful in a clinical context to know what the absolute level of blood perfusion is within a given tissue. There are numerous techniques that have been developed for this purpose over the past several decades. In some of these techniques, the coupling between vascular perfusion and local tissue temperature is applied to advantage to assess the flow through local vessels via inverse solution of equations which model the thermal interaction between perfused blood and the surrounding tissue.

Pennes [28] published the seminal work on developing a quantitative basis for describing the thermal interaction between tissue and perfused blood. His work consisted of a series of experiments to measure temperature distribution as a function of radial position in the forearms

of nine human subjects. A butt-junction thermocouple was passed completely through the arm via a needle inserted as a temporary guideway, with the two leads exiting on opposite sides of the arm. The subjects were unanesthetized so as to avoid the effects of anesthesia on blood perfusion. Following a period of normalization, the thermocouple was scanned transversely across the mediolateral axis to measure the temperature as a function of radial position within the interior of the arm. The environment in the experimental suite was kept thermally neutral during experiments. Pennes' data showed a temperature differential of three to four degrees between the skin and the interior of the arm, which he attributed to the effects of metabolic heat generation and heat transfer with arterial blood perfused through the microvasculature.

Pennes proposed a model to describe the effects of metabolism and blood perfusion on the energy balance within tissue. These two effects were incorporated into the standard thermal diffusion equation, which is written in its simplified form as:

$$\rho c \frac{\partial T}{\partial t} = \quad k \quad T + (\rho c)_b \omega_b (T_a - T) + q_{met} \qquad (37)$$

Metabolic heat generation, q_{met}, is assumed to be homogeneously distributed throughout the tissue of interest as rate of energy deposition per unit volume. It is assumed that the blood perfusion effect is homogeneous and isotropic and that thermal equilibration occurs in the microcirculatory capillary bed. In this scenario, blood enters capillaries at the temperature of arterial blood, T_a, where heat exchange occurs to bring the temperature to that of the surrounding tissue, T. There is assumed to be no energy transfer either before or after the blood passes through the capillaries, so that the temperature at which it enters the venous circulation is that of the local tissue. The total energy exchange between blood and tissue is directly proportional to the density, ρ_b, specific heat, c_b, and perfusion rate, ω_b, of blood through the tissue, and is

described in terms of the change in sensible energy of the blood. This thermal transport model is analogous to the process of mass transport between blood and tissue, which is confined primarily to the capillary bed.

A major advantage of the Pennes model is that the added term to account for perfusion heat transfer is linear in temperature, which facilitates the solution of Eq. (37). Since the publication of this work, the Pennes model has been adapted by many researchers for the analysis of a variety of bioheat transfer phenomena. These applications vary in physiological complexity from a simple homogeneous volume of tissue to thermal regulation of the entire human body (Wissler [34, 35]). As more scientists have evaluated the Pennes model for application in specific physiological systems, it has become increasingly clear that many of the assumptions foundational to the model are not valid. For example, Chato [36], Chen and Holmes [37], and Weinbaum, et al. [38-50] all demonstrated very convincingly that thermal equilibration between perfused blood and local tissue occurs in the precapillary arterioles and that by the time blood flows into vessels 60μm in diameter and smaller, the equilibration process is complete. Therefore, no significant heat transfer occurs in the capillary bed; the exchange of heat occurs in the larger components of the vascular tree. The vascular morphology varies considerably among the various organs of the body, which contributes to the need for specific models for the thermal effects of blood flow (as compared to the Pennes model that incorporates no information concerning vascular geometry). It would appear as a consequence of these physiological realities that the validity of the Pennes model is questionable.

Many investigators have developed alternative models for the exchange of heat between blood and tissue. These models have accounted for the effects of vessel size (Chato [36]: Chen and Holmes [37]; Mooibroek and Lagendijk [51]), countercurrent heat exchange (Baish [52];

Huang , et al.[53]; Keller and Seiler [54]; Mitchell and Meyers [55]; Mooibroek and Lagendijk [51]), as well as a combination of partial countercurrent exchange and bleed-off perfusion (Weinbaum and Jiji 38-50]). All of these models provided a larger degree of rigor in the analysis, but at the compromise of greater complexity and reduced generality. Some of these models have been the subject of considerable debate concerning their validity and range of appropriate application (Baish, et al. [56]; Weinbaum and Jiji [57]; Wissler [58, 59]). These studies also led to an increased appreciation of the necessity for a more explicit understanding of the local vascular morphology as it governs bioheat transfer, which has given rise to experimental studies to measure and characterize the three dimensional architecture of the vasculature in tissues and organs of interest.

It is quite interesting that, in the context of the above studies to improve on the widely applied but questioned Pennes model, the 50th anniversary of the publication of Pennes' paper was recognized recently [60]. For this occasion Wissler [59] returned to Pennes' original data and analysis and reevaluated his work. Given the hindsight of five decades of advances in bioheat transfer plus greatly improved computational tools and better constitutive property data, Wissler's analysis pointed out further flaws in Pennes' work which had not been appreciated previously. However, he also showed that much of the criticism that has been directed toward the Pennes model is not justified, in that his improved computations with the model demonstrated a good standard of agreement with the experimental data. Thus, Wissler's conclusion is that "those who base their theoretical calculations on the Pennes model can be somewhat more confident that their starting equations are valid." The quantitative analysis of the effects of blood perfusion on the internal temperature distribution in living tissue remains a topic of active research after a half century of study.

B. LIMITATIONS OF PENNES' MODEL

Pennes' model was the first major effort in quantifying the heat transfer contribution of perfusion. It was developed for describing the transverse temperature profile in the human forearm. The model is unique in that the perfusion term is very simple. The "bioheat equation" was previously shown as Eq. (37).

The limitations of this model arises from the erroneous view of the heat transfer process and its anatomical location. Chen and Holmes' analysis of blood vessel thermal equilibration lengths showed that Pennes' concept is incorrect [37]. The thermal equilibration length is defined as the length at which the difference between the blood and tissue temperature decreases to 1/e of the initial value. They indicated that thermal equilibration occurs predominantly within the terminal arterioles and venules, and that blood is essentially equilibrated prior to the capillaries. In considering the contribution of perfusion as a non-directional term, the directional convective mechanism is neglected. Nor does the model account for specific vascular architecture such as counter-current arteries and veins. The limitations of Pennes' model have motivated subsequent investigators to develop their own models.

Despite its erroneous concept, the perfusion term of Pennes' model has been widely used, and found to be valid for situations other than the forearm. Its wide usage has been mainly due to its simplicity of implementation, especially in analyses where a closed form analytical solution is sought [22, 61]. Investigators have obtained good temperature predictions for the following circumstances: 1) the porcine kidney cortex in the absence of large vessels (diameter > 300 μm) [62], 2) the rat liver [5, 22], and 3) the capillary bleed-off from large vessels [42]. In the last case, Charny compared Weinbaum-Jiji's counter-current model and Pennes' model against the experimental results of Pennes. The simulations found that Pennes' model is valid in the initial

branchings of the largest microvessels from the counter-current vessels (diameter > 500 μm) in deep tissue. In this case, the microvessel blood temperature is close to arterial temperature. Arkin *et al.* [63] provides an explanation of the inconsistencies between the two anatomical sites. They suggest that since blood typically travels down successive generations of the vascular branches before equilibrating with the tissue temperature, Charny's claim actually refers to the collective contribution of numerous smaller thermally significant vessels in a region dominated by the large microvessels. The distinction of being thermally significant is based upon the ratio of thermal equilibration length to actual vessel length (ε):

$$\varepsilon = \frac{L_e}{L} \tag{38}$$

Along with Xu's observations in porcine kidney [62], Pennes' model appears to be applicable to regions where the vasculature comprises of numerous small thermally significant vessels (ε ≈ 1).

C. CONTINUUM MODELS

Among the continuum formulations of bioheat transfer, the Chen-Holmes model is the most developed. Prior to Chen-Holmes, continuum formulations by Wulff [64] and Klinger [65] addressed the isotropicity of Pennes' perfusion term. However, they did not challenge the Pennes' concept of the site of heat exchange. Chen and Holmes [37] formulated their model after analyzing the significance of blood vessel thermal equilibration length. Through this analysis, they quantitatively showed that the major heat transfer processes occur in the 50 to 500 μm diameter vessels and refuted Pennes' paradigm. In their model, they proposed that larger vessels be modeled separately from smaller vessels and tissue. Larger vessels were distinguished using the ratio of equilibration length to actual vessel length of about one (ε ≈ 1) as the criteria. The

smaller vessels and tissue were then modeled as a continuum. In a differential control volume of this continuum, they further separated solid tissue from the blood within the vascular space (Fig. 2).

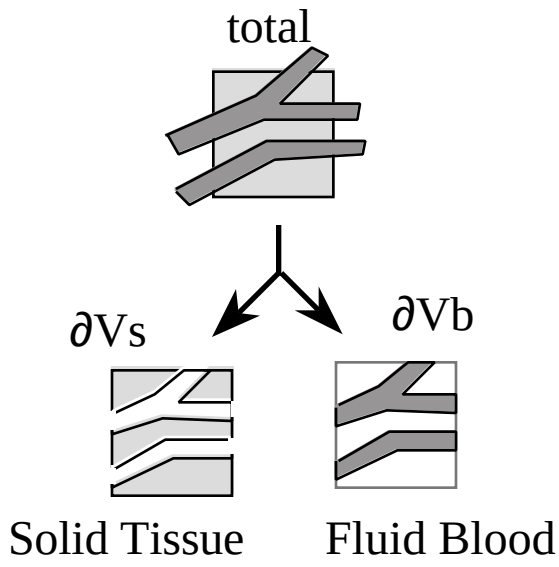

Figure 2. Schematic Representation of Tissue Control Volume as Used by Chen-Holmes [8]

Subsequently, the heat transfer mechanisms can be divided into the contributions from 1) non-equilibrated blood in the thermally significant vessels, 2) blood that has equilibrated with the surrounding tissue, and 3) nearly equilibrated blood. The perfusion term of Pennes is then replaced with three terms.

$$\rho c \frac{\partial T}{\partial t} = \quad k \quad T + (\rho c)_b \omega^* \left(T_a^* - T\right) - (\rho c)_b \vec{u} \quad T + \quad k_p \quad T + q_m \qquad (39)$$

The second through the fourth term on the right hand side arise from each of the three categories described above. The second term, $(\rho c)_b \omega^* \left(T_a^* - T\right)$, is similar to Pennes except the perfusion and the arterial temperature is specific to the volume being considered. The $(\rho c)_b \vec{u} \quad T$ term is

a directional convective term due to the net flux of equilibrated blood. Finally, the $k_p \nabla T$ term is to account for the contribution of the nearly equilibrated blood in a tissue temperature gradient. The nearly equilibrated blood contributes to small temperature fluctuations within the tissue and the effect is modeled as a tensor "perfusion conductivity"

$$k_p = n(\rho c)_b \pi r_b^2 \bar{V} \cos^2 \gamma \sum_{i=1}^{\infty} \frac{L_e}{L_e^2 \beta_i^2 + 1} \qquad (40)$$

which is a function of local average blood flow velocity vector within the vessel ($\bar{V}$), relative angle (γ) between blood vessel direction and the tissue temperature gradient, the number of vessels (n), and vessel radius (r_b). The Fourier integral spectral wave number (β) can be approximated as the inverse of vessel length. The contribution of this conductivity is minimal except when vessels with large equilibration lengths are considered. However, for this situation, Chen and Holmes recommend that these vessels be treated separately. The assumptions which were made for their model include: 1) neglecting the mass transfer between vessel and tissue space, and 2) treating the thermal conductivity and temperature within the tissue-blood continuum as that of the solid tissue since the vascular volume is much smaller than that of the solid tissue.

The limitation of this model is that given the detail required, the model is not easy to implement. Also, the perfusion conductivity term is difficult to evaluate, and distinction within the continuum model is not well defined. Furthermore, the model does not explicitly address the effect of closely spaced counter-current artery-vein pairs. This model has been applied to the porcine kidney and was found to predict temperatures similar to Pennes model, and thus, given the simplicity of the latter, Xu *et al.* [62] recommended that Pennes be used. Arkin *et al.* [63]

claim that the Chen-Holmes model can be essentially applied to the same tissue region as that for Pennes.

D. VASCULATURE-BASED MODELS

1. Weinbaum-Jiji-Lemons [38-50]

The modeling of counter current vasculature, which was not explicitly addressed by the Chen-Holmes model, developed separately from that of the continuum models. Bazett *et al.* [66] initially presented the counter-current structure from observations of large arteries and veins in human limbs. The first major quantitative analysis was presented by Mitchell and Myers [55]. It was then followed by the work of Keller and Seiler [54], which became the predecessor to the Weinbaum-Jiji models. In 1979, Weinbaum and Jiji [43] proposed the initial model of the artery-vein pair as two parallel cylinders of equal diameters with collateral bleedoff in the plane normal to the cylinders. The anatomical configuration is a schematic of an artery and vein pair with branches to the peripheral skin layer (Fig. 3).

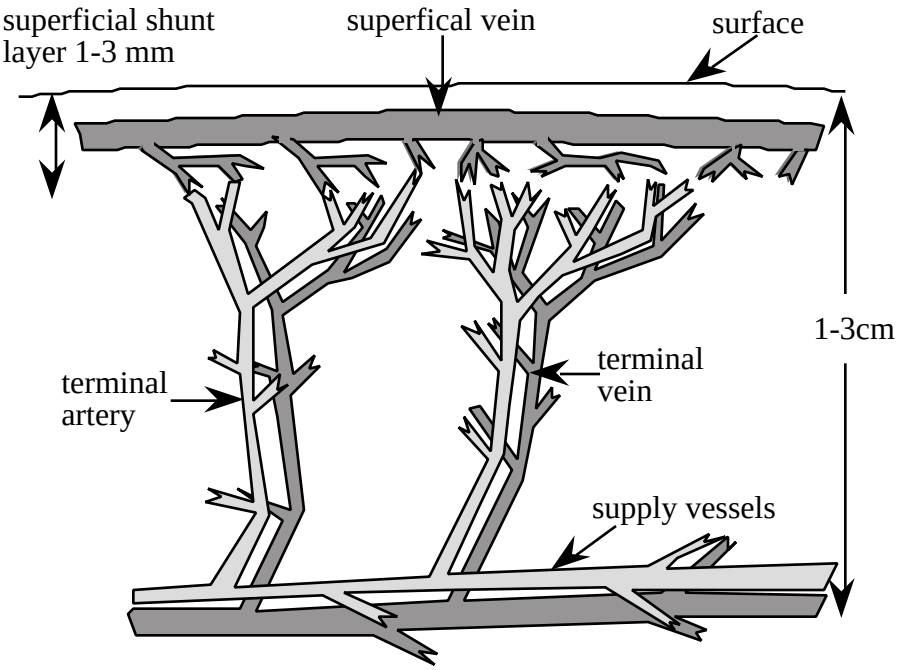

Figure 3. Schematic of Artery and Vein Pair in Peripheral Skin Layer [43]

The contribution of perfusion to heat transfer in tissue was treated as heat transfer in a porous medium. It was considered as a unidirectional convective term normal to the artery-vein pair. Knowledge of vessel density, diameter, and blood velocity was required at the different blood vessel generations.

In 1984, they presented a more thorough model based upon anatomical observations with Lemons [38, 39]. This model analyzed three tissue layers of a limb: 1) deep, 2) intermediate, and 3) superficial or cutaneous. For the counter current structure of the deep tissue layer, they proposed a system of three coupled equations:

$$(\rho c)_b \pi r_b^2 \overline{V} \frac{dT_a}{ds} = -q_a \qquad (41)$$

$$(\rho c)_b \pi r_b^2 \bar{V} \frac{dT_v}{ds} = -q_v \quad (42)$$

$$\rho c \frac{\partial T}{\partial t} = k \nabla T + n g (\rho c)_b (T_a - T_v) - n \pi r_b^2 (\rho c)_b \bar{V} \frac{d(T_a - T_v)}{ds} + q_m \quad (43)$$

The first two equations describe the heat transfer of the thermally significant artery and vein, respectively. The third equation refers to the tissue surrounding the artery-vein pair. For this equation, the middle two right-hand side terms represent the capillary bleed-off energy exchange, and the net heat exchange between the tissue and artery-vein pair, respectively. The capillary bleed-off term is similar to Pennes' perfusion term except the bleed-off mass flow (g) is used. Their analysis showed that the major heat transfer is due to the imperfect counter-current heat exchange between artery-vein pairs. They quantified the effect of perfusion bleed-off associated with this vascular structure, and showed that Pennes' perfusion formulation is negligible due to the temperature differential.

Assumptions include the following: 1) neglecting the lymphatic fluid loss so that the mass flow rate in the artery is equal to that of the vein, 2) spatially uniform bleed-off perfusion, 3) heat transfer in the plane normal to the artery-vein pair is greater than that along the vessels (in order to apply the approximation of superposition of a line sink and source in a pure conduction field), 4) a linear relationship for the temperature along the radial direction in the plane normal to the artery and vein, 5) the artery-vein border temperature equals the mean of the artery and vein temperature, and 6) the blood exiting the bleed-off capillaries and entering the veins is at the venous blood temperature. The last assumption has drawn criticism based on studies that indicate the temperature to be closer to tissue [58, 63]. Limitations of this model include the difficulty of implementation, and that the artery and vein diameters are identical. Both these issues have lead to the development of the models described in subsequent sections.

Studies using this model have been applied to the peripheral muscle tissue of a limb [44-46], and the model is accepted as valid for vasculature with diameters < 300 μm and $\varepsilon < 0.3$ [63].

2. Simplified Weinbaum-Jiji (W-J) [40]

In response to the criticism that their previous model is difficult and complex to apply, Weinbaum and Jiji simplified the three equation model to a single equation.

$$\rho c \frac{\partial T}{\partial t} = \frac{\partial}{\partial x}\left(k_{eff} \frac{\partial T}{\partial x}\right) + q_{met} \qquad (44)$$

In their simplification, they derived an equation based on the temperature of tissue only. The imperfect counter-current heat exchange is embodied in an effective conductivity tensor term.

$$k_{eff} = k\left(1 + \frac{n\left[(\rho c)_b \pi r_b^2 \bar{V} \cos\gamma\right]^2}{\sigma_\Delta \; k^2}\right) + q_{met} \qquad (45)$$

The k_{eff} term has similar parameters to the tissue and artery-vein pair heat exchange term in Eq. (45), and a shape factor term (σ_Δ). In order to eliminate the blood temperature from their previous formulation, two major assumptions (the closure conditions) were used:

1) the mean tissue temperature = $(T_a + T_v)/2$, and

2) heat from paired artery is mostly conducted to the corresponding vein:

$$q_a \approx q_v \approx \sigma_\Delta \, k \, (T_a - T_v). \qquad (46)$$

Both these assumptions were based upon studies in rabbit thigh muscle from their previous formulation. However, to respond to criticism of these assumptions, they performed further mathematical analysis on ε and provided insights into the limits for applying these assumptions [47]. An obvious limitation of this model is that the local temperatures along the counter-current artery and vein cannot be calculated. Another limitation is that the model is applicable only in

situations where $\frac{L_e}{L} << 1$. In the example of analyzing the peripheral tissue in the arm, L is equal to the characteristic radius of the arm [48]. Weinbaum and Lemons [48] admit that this assumption breaks down under the following conditions: 1) if blood flow rates significantly increased in the larger vessel pairs of the peripheral tissue layer, and 2) if deeper muscle tissue, where the diameter of the counter-current pair vessels are less than 300 μm, are included. This model has been tested in the porcine [62] and canine kidney [67], and continues to be verified by the Weinbaum group [41, 50] and other investigators [68].

3. Small Artery Model [69, 70]

The Small Artery was developed by Anderson in studies of the canine kidney cortex. The model considers the energy balance in a control volume (i, j, k) which contains either an arterial (Q_a) or venous (Q_v) vessel. For a volume with an artery parallel to the 'z' coordinate axis, the equation is

$$Q_a = N(VA)_a(\rho c)_b(1+\lambda-2\lambda\xi)\left(\frac{T_z - T_{z-\Delta z}}{\Delta z}\right) \quad (47).$$

For a volume with a vein:

$$Q_v = M(VA)_v(\rho c)_b(1+\lambda-2\lambda\xi)\left(\frac{T_{z+\Delta z} - T_z}{\Delta z}\right) \quad (48).$$

Where N and M are the density of the interlobular arteries and veins in the kidney cortex, respectively. ξ refers to the fraction of the total interlobular artery flow within the control volume; in the kidney cortex, $\xi = 1$ at the cortico-medullary junction and decreases to $\xi = 0$ at the outer capsule. The total flow within this region accounts for bleed-off from the interlobular arteries through the λ term, where $\lambda = 1$ represents complete bleed-off. The discrete

representation provides for straightforward numerical implementation when the vessel density within the tissue region of interest is known. Model assumptions include: 1) thermal equilibration length within the volume is much less than vessel length, 2) a linear relation between the effect of bleed-off on arterial flow and location along the length of the vessel, 3) bleed-off is modeled as change in the arterial flow, 4) bleed-off heat transfer is negligible, and 5) no major thermally significant vessels (i.e., $\varepsilon << 1$) in the region of interest. In its initial formulation, arbitrarily oriented vessels which would cause more than one vessel to occupy a control volume were not considered. Branching vessels are also not addressed. Even though this is not an inherent limitation of the model, implementation would be more difficult. Due to its discrete representation, the model cannot solve the inverse problem. The model has been shown to be valid in the canine kidney cortex where there is uniformly oriented counter-current artery vein architecture of 70 μm diameters.

E. HYBRID MODELS

The lack of an encompassing model which can account for the various tissue structures have lead researchers to propose and apply hybrid models. The substantial amount of efforts related to the application and investigation of the major models discussed have shown that no one model applies to all the different vascular structures in tissue [58, 63]. Wissler [58, 59] points to the unlikelihood of a single equation being able to provide a complete description of the heat transfer process in tissue, and thus suggests the use of a combination of equations. The realization of this suggestion is found in Charny's work [42] in which W-J's and Pennes' model are used to describe peripheral and deep muscle tissue, respectively. When the applicability of each of the major models have been conclusively defined, an algorithm which would enable

users to arrive at the appropriate choice of equations given the tissue vasculature of interest would be beneficial.

The applicability of the models discussed requires an understanding of the validity and development of each model. A comparison of the models discussed has been summarized by Charney [33].

F. THERMAL MEASUREMENTS OF PERFUSION

1. Introduction

Perfusion, the transmission of blood in the microcirculation, is an important factor in surgery, tissue transplants, heart disease and cancer therapy. Despite its importance, no clinical method of measuring perfusion is currently available for a majority of applications. One technique that shows considerable promise involves the use of self-heated thermistors [6-13]. In this method, a miniature thermistor (0.5 to 2.5 mm diameter) is placed invasively in the tissue of interest and heated with a predetermined applied power. Since both tissue conduction and perfusion act to carry heat away from the thermistor, the resulting volumetric-average temperature rise in the thermistor bead, ΔT, is related to both the tissue thermal conductivity and perfusion. By knowing the intrinsic tissue conductivity and the apparent conductivity of the tissue (due to both blood flow and conduction), the perfusion rate can be calculated.

At least two difficulties exist with this technique. The first is that the intrinsic tissue conductivity of perfused tissue must be known in order to calculate the perfusion rate. Although one could stop the blood flow to a tissue and measure its conductivity, this is clearly not desirable, nor is it always practical. In order to overcome this problem, Holmes and Chen have proposed techniques that measure perfusion without interrupting blood flow [13, 20].

2. Perfusion Resolution

The perfusion resolution, δw, is defined as the smallest change in perfusion that can be detected by the instrument. It can be determined theoretically:

$$\delta w = \delta k \bullet \frac{\partial w}{\partial k} = \delta k \bullet c_{15} \tag{49}$$

For the constant temperature heating technique using a P60 thermistor, δk is about 0.02 mW/cm-°C, and the sensitivity is about 100 (mL/100g-min)/(mW/cm-°C). Using Eq. (49) gives a perfusion resolution of about 2 mL/100g-min. Due to fluctuations in the baseline tissue temperature, the practical resolution is about 10 mL/100g-min. There are so many experimental and tissue variables that it is extremely important to test these techniques in preparations where the perfusion is known.

3. Measurement Volume

The measurement volume of a thermistor is a complex function of many factors, including the perfusion rate and vascular anatomy of the tissue of interest. One problem with small thermistors is their small measurement volume. A boundary layer (decoupler) between the thermistor and the tissue causes a significant measurement error. This unwanted boundary layer is often caused by the probe itself during insertion. The larger probes exhibit a smaller error, but are likely to cause a larger decoupler because of the increased trauma during insertion.

4. Temperature Dependence of Perfusion

Perfusion depends on a wide variety of factors, some local to the tissue (pH, temperature, O_2), some which are external but directly control local flow (parasympathetic, hormones), and some which indirectly affect local flow (heart rate, blood pressure, skin temperature, needs of other organs. A simple experiment studied the effect of local tissue temperature on muscle perfusion. The constant ΔT method was used to measure perfusion in an anesthetized rat. The

muscle temperature was manipulated by placing the hindlimb into a water bath. Insulation was carefully placed so as to minimize changes to the body temperature. The rectal and neck temperatures were constant while the muscle in the hindlimb was heated. Figure 4 shows the perfusion as a function of tissue temperature for a typical experiment. The dip in perfusion as a function of temperature as shown in Figure 4 consistently occurred, but did not always occur at the same temperature. This dip may be due to an anastomotic shunt attempting to regulate the core body temperature.

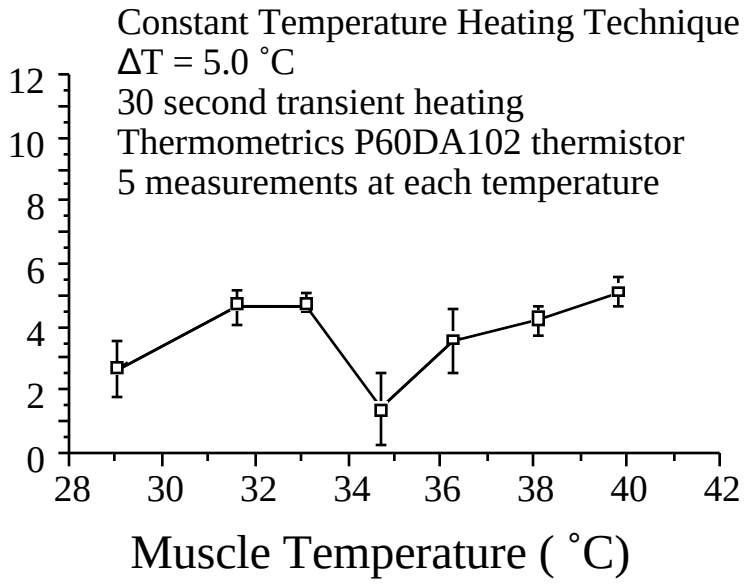

Figure 4. Perfusion versus muscle temperature during a typical experiment.

Figure 5 presents the averaged results for 10 rats. Because the dip occurred at different temperatures for the various rats, it does not appear in the average. The large standard deviations are due to perfusion differences from one rat to the next. A linear fit to this averaged data gives the following approximation.

$$w = 1.9720 (1 + 0.059 T) \qquad (50)$$

where w has units of mL/100g-min and T has units of ˚C.

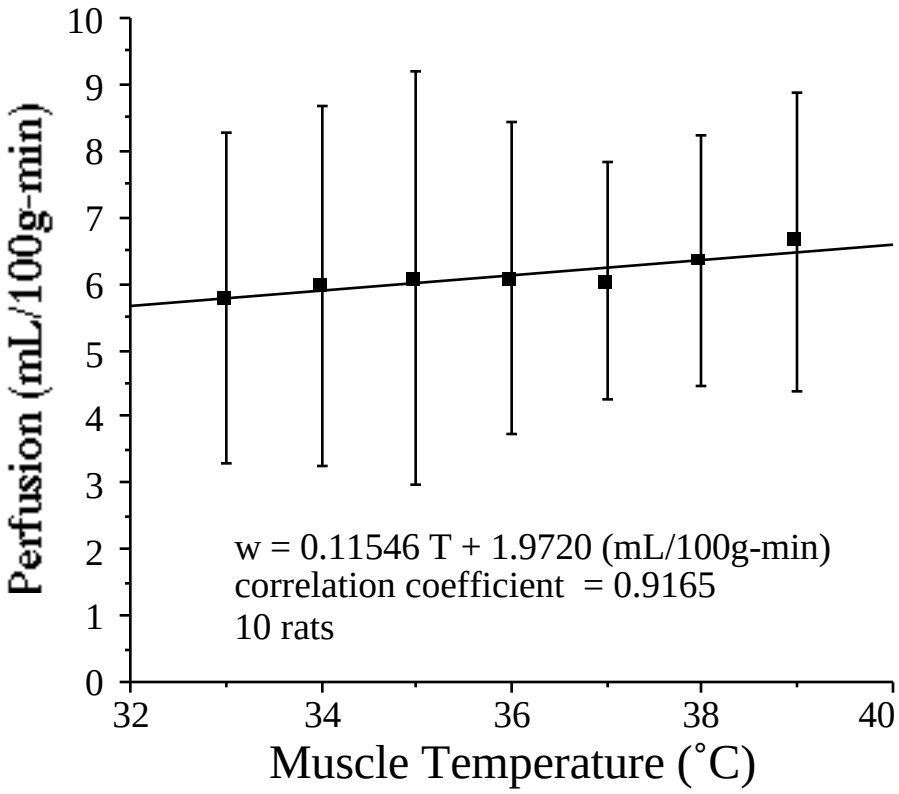

Figure 5. Perfusion versus muscle temperature averaged over 10 experiments.

Yuan et al. [71] measured perfusion and temperatures at various locations within each of the four canine prostates subjected to a transurethral microwave thermal source. The total number of the perfusion sampling points coupled with temperature is 15. Colored microspheres were used to measure perfusion due to its simplicity compared with radioactively-labeled microspheres and because the microsphere trapping method is regarded as a standard. Temperatures were measured using miniature thermistors. The prostate temperatures were raised to 40 ~ 45 ^{0}C by 5W step increments of the microwave power at hourly intervals to 15W. Temperatures and perfusion were measured at baseline, and at the beginning and end of each heating interval. Thus, the periods between perfusion samples were approximately either 5 or 60

minutes. Under baseline conditions, the temperature fluctuations within the prostate were approximately ± 0.3 ^{0}C. A relative dispersion estimate of 15% was derived from one dog for the fluctuations in baseline perfusion. Thus, changes in absolute perfusion and temperature greater than 15% and 0.3 ^{0}C, respectively, were considered to be substantial changes.

As heating progressed, a variety of substantial changes were observed, but no uniform pattern emerged. However, the measurements included changes typically expected for hyperthermia: 1.) an initial perfusion increase associated with elevating the baseline temperature, 2.) a perfusion return towards baseline after this initial increase, and 3.) a dramatic increase in perfusion at elevated temperatures. The initial perfusion increases were observed in three dogs when the temperatures exceeded 38 ± 3 ^{0}C (mean ± 1 s.d., N = 8). The perfusion increased 34% from a baseline value of 0.59 ± 0.26 ml/g-min over a temperature rise of 1.7 ± 1.3 ^{0}C. Half of the measurements in the three dogs subsequently showed a decrease in perfusion ranging from 16% to 25%. In two dogs, dramatic perfusion increases as high as 364% were observed with a corresponding decrease in tissue temperature.

The mean perfusion and temperature measured from all dogs at similar instances during the experimental protocol were calculated. The following figure shows the changes as the experiment progressed from baseline conditions:

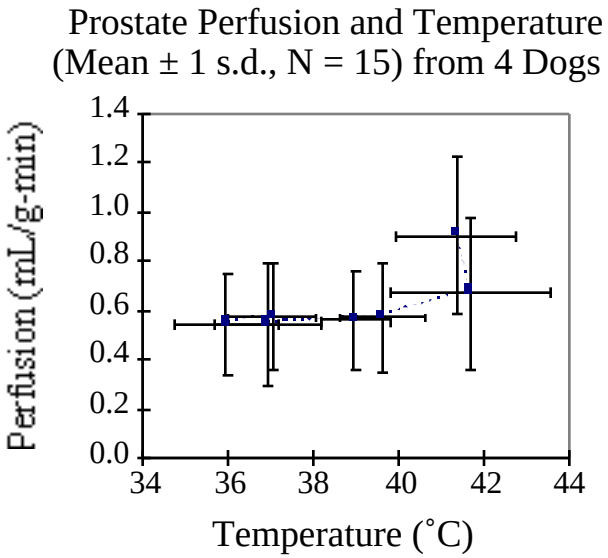

Figure 6. Perfusion versus prostate temperature [71].

The mean behavior indicates no substantial change in perfusion until the tissue temperature exceeded 39.6 ^{0}C, after which the perfusion increased 17%. This occurred over a 5 minute period as the nominal microwave power was stepped from 10W to 15W. The perfusion increased another 35% when the tissue temperature exceeded 41.7 ^{0}C, and appeared to affect a slight lowering of tissue temperature.

Xu et al. [72] measured perfusion using the pulse-decay self-heated thermistor technique [13, 20] in these dog prostates during the same transurethral microwave hyperthermia treatments. Interestingly in the exact same dogs at roughly the same locations, the perfusion response to temperature measured with the thermal technique was roughly linear with temperature as shown in Figure 7.

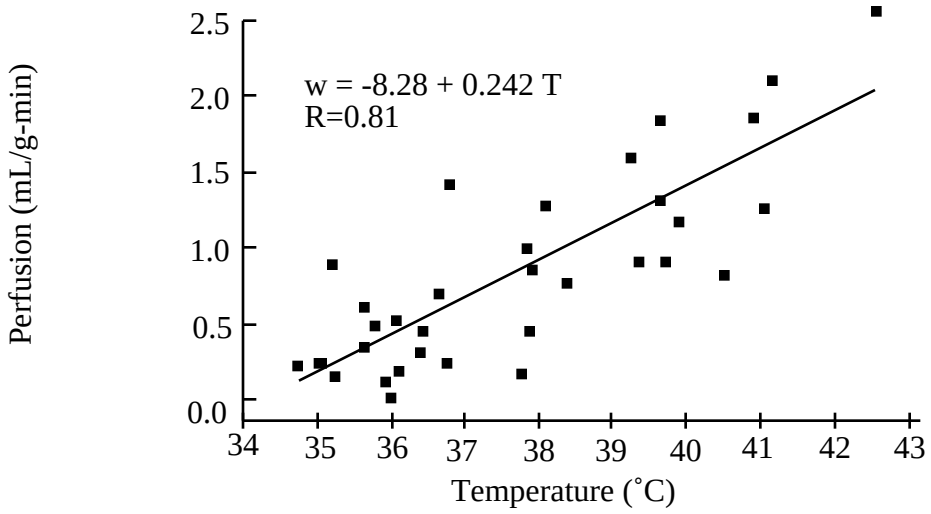

Figure 7. Perfusion versus prostate temperature [72].

The interdependence between perfusion and temperature was observed in these studies. Most notably, a decrease in tissue temperature associated with a dramatic increase of perfusion. Such changes have been modeled previously with Pennes' bioheat equation using assumed perfusion values and changes for the prostate. The data from this study will provide more realistic estimates of perfusion values and thermoregulation models in hyperthermic canine prostates. Two hypotheses exist that explain the differences between the perfusion responses to hyperthermia as measured by microspheres and the thermal decay probe. The first possibility is that one or both methods have significant measurement errors. A second possibility is that perfusion as measured by spheres trapped in the capillaries is a different parameter than perfusion as measured by enhanced heat transfer within the 70 to 200 μm diameter vessels.

X. ACKNOWLEDGEMENTS (Valvano)

The perfusion measurements were supported in part by a grant from Urologix Inc. This chapter was prepared in part with the support of NIH grant #1 R01 HL56143-01. The sections on convective heat transfer and thermal properties of swine myocardium were derived from Naresh

C. Bhavaraju's soon to be completed Ph.D. dissertation. In a similar fashion, the sections on thermal models and microsphere perfusion measurements in the canine prostate were derived from David Yuan's soon to be completed Ph.D. dissertation.

XI. REFERENCES (Valvano)

[3] Chato, J.C., 1968, "A Method for the Measurement of Thermal Properties of Biologic Materials," *Symposium on Thermal Problems in Biotechnology*, ASME, New York, LCN068-58741, pp. 16-25.

[4] Balasubramaniam, T.A., Bowman, H.F., 1977, "Thermal Conductivity and Thermal Diffusivity of Biomaterials: A Simultaneous Measurement Technique", *J. of Biomechanical Eng*., Vol. 99, pp. 148-154.

[5] Valvano, J.W., *et al.*, 1984, "An Isolated Rat Liver Model for the Evaluation of Thermal Techniques to Measure Perfusion," *J. of Biomech. Eng.* Vol. 106, pp. 187-191.

[6] Arkin, H., *et al.*, 1986, "Thermal Pulse Decay Method for Simultaneous Measurement of Local Thermal Conductivity and Blood Perfusion: A Theoretical Analysis," *J. of Biomechanical Engineering*, Vol. 108, pp. 208-214.

[7] Kress, R., 1987, "A Comparative Analysis of Thermal Blood Perfusion Measurement Techniques," *J. of Biomechanical Engineering*, Vol. 109, pp. 218-225.

[8] Patel, P.A., *et al.*, 1987, "A Finite Element Analysis of a Surface Thermal Probe," *Thermodynamics, Heat, and Mass Transfer in Biotech.*, ASME Winter Annual Meeting, Boston, HTD-Vol. 90, BED. Vol. 5, edited by Diller, pp. 95-102.

[9] Bowman, H.F., 1985,"Estimation of Tissue Blood Flow", in Heat Transfer in Medicine and Biology, Plenum Pub., Shitzer and Eberhart (ed.), pp. 193-230.

[10] Chato, J.C., 1985, "Measurement of Thermal Properties of Biological Materials", in Heat Transfer in Medicine and Biology, Plenum Pub., Shitzer and Eberhart (ed.), pp. 167-192.

[11] Valvano, J.W., *et al.*, 1985, "Thermal Conductivity and Diffusivity of Biomaterials Measured with Self-Heated Thermistors," *Intern. J. of Thermophysics*, Vol. 6, pp. 301-311.

[12] Valvano, J.W., Chitsabesan, B., 1987, "Thermal Conductivity and Diffusivity of Arterial Wall and Atherosclerotic Plaque," Lasers in the Life Sciences, Vol. 1, pp. 219-229.

[13] Holmes, K.R., Chen, M.M., 1980, "*In vivo* Tissue Thermal Conductivity and Local Blood Perfusion Measured with Heat Pulse-decay Method", *Advances in Bioeng.*, pp. 113-115.

[14] Touloukian, Y.S., et al., 1970, Thermophysical Properties of Matter: Thermal Conductivity, IFI/ Plenum, New York, Vo1. 3, pg. 120, pg. 209.

[15] Touloukian, Y.S., et al., 1970, Thermophysical Properties of Matter: Thermal Conductivity, IFI/ Plenum, New York, Vo1. 3, preface.

[16] Touloukian, Y.S., et al., 1973, Thermophysical Properties of Matter: Thermal Diffusivity, IFI/ Plenum, New York, Vo1. 10, pp.15a-42a.

[17] Eckert, E.R,G., and Drake, R.M. Jr., 1959, Heat and Mass Transfer, 2nd Edition, McGraw-Hill Book Company, New York.

[18] Duck, F.A., 1991, Physical Properties of Tissue: A Comprehensive Reference Book, Academic Press, London.

[19] Chen, M.M., et al., 1981, "Pulse-Decay Method for Measuring the Thermal Conductivity of Living Tissue," *J. of Biomech. Eng.* Vol. 103, pp. 253-260.

[20] Holmes, K.R., Chen, M.M., 1983, "Local Tissue Heating, Microbead Pulse Decay Technique for Heat Transfer Parameter Evaluation", Measurement of Blood Flow and Local Tissue Energy Production by Thermal Methods, Muller-Schenburg (ed.), Thieme-Stratton Inc., New York, pp. 50-56.

[21] Valvano, J.W., *et al.*, 1983, "A Finite Element Analysis of Self-heated Noninvasive Thermistors", *Advances in Bioengineering*, American Society of Mechanical Engineers.

[22] Valvano, J.W., *et al.*, 1984, "The Simultaneous Measurement of Thermal Conductivity, Thermal Diffusivity and Perfusion in Small Volume of Tissue," *J. of Biomech. Eng.* Vol. 106, pp. 192-197.

[23] Valvano, J.W., Badeau, A.F., and Pearce, J.A., 1987b, "Simultaneous Measurement of Intrinsic and Effective Thermal Conductivity," *Heat Transfer in Bioengineering and Medicine*, ASME Winter Annual Meeting, Boston, HTD-Vol 95, BED. Vol. 7, edited by Chato, Diller, Diller, Roemer, pp. 31-36.

[24] Patel, P.A., *et al.*, 1987b, "A Self-Heated Thermistor Technique to Measure Effective Thermal Properties from the Tissue Surface", *J. of Biomech. Eng.* Vol. 109, pp. 330-335.

[25] Patel, P.A., Valvano, J.W., Hayes, L.J., 1987c, "Perfusion Measurement by a Surface Thermal Probe," IEEE Engineering in Medicine and Biology, Boston.

[26] Walsh, J.T., 1984, *A Noninvasive Thermal Method for the Quantification of Tissue Perfusion*, M.S. Thesis, Mass. Inst. of Tech., Cambridge, MA.

[27] Patera, *et al.*, 1979, "Prediction of Tissue Perfusion from Measurement of the Phase Shift between Heat Flux and Temperature", *AMSE*, Paper #79-WA/HT-71.

[28] Pennes, H.H., 1948, "Analysis of Tissue and Arterial Blood Temperature in the Resting Human Forearm," *J. of Applied Physiology*, Vol. 1, pp. 93-102.

[29] Rastorguev, Y.L., Ganiev, Y.A., 1966, "Thermal Conductivity of Aqueous Solutions or Organic Materials", Russian Journal of Physical Chemistry, Vol. 40, pp. 869-871., Y.S., et al., 1970a, Thermophysical Properties of Matter: Thermal Conductivity, IFI/ Plenum, New York, Vo1. 1, pp. 13a-25a.

[30] Valvano, J.W., 1988, "Low Temperature Tissue Thermal Properties", *Low Temperature Biotechnology*, American Society of Mechanical Engineers Heat Transfer Division, Vol. 98, pp. 331-346.

[31] Spells, K. E., 1960, "The thermal conductivities of some biological fluids", Phys. Med. Biol., 5, pp. 139-153.

[32] Cooper, T. E., and Trezck, G. J., " Correlation of thermal properties of some human tissues with water content", Aerospace. Med., 42, pp. 24-27, 1971.

[33] Charney, C.K., Mathematical models of bioheat transfer, *Adv. Heat Trans.*, 22, 19-155, 1992.

[34] Wissler, E., "Steady state temperature distribution in man," *J. Appl. Physi*ol.,, 16, 734-740, 1961.

[35] Wissler, E.H., Mathematical simulation of human thermal behavior using whole-body models, *Heat Transfer in Medicine and Biology*, *Vol. 1*, Shitzer, A. and Eberhart, R.C., Eds., Plenum Press, New York, 1985, 325-373.

[36] Chato, J.C., Heat transfer to blood vessels, *J. Biomech. Engr.*, 102, 110-118, 1980.

[37] Chen, M.M. and Holmes, K.R., "Microvascular contributions in tissue heat transfer," *Annals NY Acad. Sci*, 335, 137-150, 1980.

[38] S. Weinbaum, L. Jiji, and D.E. Lemons, "Theory and Experiment for the Effect of Vascular Temperature on Surface Tissue Heat Transfer – Part 1: Anatomical Foundation and Model Conceptualization," *ASME J. Biomech. Eng.*, 106: 246-251, 1984.

[39] S. Weinbaum, L. Jiji, and D.E. Lemons, "Theory and Experiment for the Effect of Vascular Temperature on Surface Tissue Heat Transfer – Part 2: Model Formulation and Solution," *ASME J. Biomech. Eng.*, 106: 331-341, 1984.

[40] S. Weinbaum, and L. Jiji, “A New Simplified Bioheat Equation for the Effect of Blood Flow on Average Tissue Temperature,” *J. of Biomech. Eng.*, 107: 131-139, 1985.

[41] L. Zhu, D.E. Lemons, and S. Weinbaum, "A New Approach for Predicting the Enhancement in the Effective Conductivity of Perfused Tissue due to Hyperthermia," *ASME Winter Annual Meeting*, HTD 288: 37-43, 1994.

[42] C.K. Charny, S. Weinbaum, and R.L. Levin, "An Evaluation of the Weinbaum-Jiji Bioheat Equation for Normal and Hyperthermic Conditions," *ASME J. Biomech. Eng.*, 112: 80-87, 1990.

[43] S. Weinbaum, and L.M. Jiji, "A Two Phase Theory for the Influence of Circulation on the Heat Transfer in Surface Tissue," *ASME Proc.: Advances in Bioengineering*, M.K. Wells, ed., WA/HT-72: 179-182, 1979.

[44] Z. Dagan, S. Weinbaum, and L.M. Jiji, "Parametric Study of the Three Layer Microcirculatory Model for Surface Tissue Energy Exchange," *ASME J. Biomech. Eng.*, 108: 89-96, 1986.

[45] W.J. Song, S. Weinbaum, and L.M. Jiji, "A Combined Macro and Microvascular Model for Whole Limb Heat Transfer," *ASME J. Biomech. Eng.*, 110: 259-267, 1988.

[46] W.J. Song, S. Weinbaum, and L.M. Jiji, "A Theoretical Model for Peripheral Heat Transfer Using the Bioheat Equation of Weinbaum and Jiji," *ASME J. Biomech. Eng.*, 109: 72-78, 1987.

[47] S. Weinbaum, and L.M. Jiji, "The Matching of Thermal Fields Surrounding Countercurrent Microvessels and the Closure Approximation in the Weinbaum-Jiji Equation," *ASME J. Biomech.*, 111: 271-275, 1989.

[48] S. Weinbaum, and D.E. Lemons, "Heat Transfer in Living Tissue: The Search for a Blood-Tissue Energy Equation and the Local Thermal Microvascular Control Mechanism,"*BMES Bull.*, 16(3): 38-43, 1992.

[49] M. Zhu, S. Weinbaum, and D.E. Lemons, "On the Generalization of the Weinbaum-Jiji Equation to Microvessels of Unequal Size: The Relation Between the Near Field and Local Average Tissue Temperatures," *ASME J. Biomech. Eng.*, 110: 74-81, 1988.

[50] D.E. Lemons, S. Weinbaum, and L.M. Jiji, "Experimental Studies on the Role of the Micro and Macro Vascular System in Tissue Heat Transfer," *Am J. Physiol.*, 253: R128, 1987.

[51] Mooibroek, J. and Lagendijk, J.J.W., A fast and simple algorithm for the calculation of convective heat transfer by large vessels in 3-dimensional inhomogeneous tissue, *IEEE Trans. Biomed. Engr.*, 38, 490-501, 1991.

[52] Baish, J.W., Heat transport by countercurrent blood vessels in the presence of an arbitrary temperature gradient, *J. Biomech. Engr.*, 112, 207-211, 1990.

[53] Huang, H.W., Chen, Z.P., and Roemer, R.B., A counter current vascular network model of heat transfer in tissues, *J. Biomech. Engr.*, 118, 120-129, 1996.

[54] Keller, K.H. and Seiler, L., An analysis of peripheral heat transfer in man, *J. Appl. Physiol.*, 30, 779, 1971.

[55] Mitchell, J.W. and Myers, G.E., An analytical model of the countercurrent heat exchange phenomena, *Biophys. J.*, 8, 897-911, 1968.

[56] Baish, J.W., Ayyaswamy, P.S., and Foster, K.R., Heat transport mechanisms in vascular tissues: a model comparison, *J. Biomech. Engr.*, 108, 324-331, 1986.

[57] Weinbaum, S. and Jiji, L.M., Discussion of papers by Wissler and Baish *et al.* concerning the Weinbaum-Jiji bioheat equation, *J. Biomech. Engr.*, 109, 234-237, 1987.

[58] Wissler, E.H., Comments on Weinbaum and Jiji's discussion of their proposed bioheat equation, *J. Biomech. Engr.*, 109, 355-356, 1987.

[59] Wissler, E.H., Pennes' 1948 paper revisited, *J. Appl. Physiol.*, 85, 35-41, 1998.

[60] Pennes, H.H., Analysis of tissue and arterial blood temperatures in the resting forearm, *J. Appl. Physiol.*, Vol. 1, pp. 93-122, 1948 (republished for fiftieth anniversary issue of *J. Appl. Physiol*, 85, 5-34, 1998).

[61] H.W. Huang, C.L. Chan, and R.B. Roemer, "Analytical Solutions of Pennes Bioheat Transfer Equation with a Blood Vessel," *ASME J. Biomech. Eng.*, 116: 208-212, 1994.

[62] L.X. Xu, M.M. Chen, K.R. Holmes, and H. Arkin, "The Evaluation of the Pennes, the Chen-Holmes, the Weinbaum-Jiji Bioheat Transfer Models in the Pig Kidney Cortex," *ASME WAM Proc.*, HDT 189: 15-21, 1991.

[63] H. Arkin, L.X. Xu, and K.R. Holmes, "Recent Developments in Modeling Heat Transfer in Blood Perfused Tissues," *IEEE Trans. Biomed. Eng.*, 41(2): 97-107, 1994.

[64] W. Wulff, "The Energy Conservation Equation for Living Tissue," *IEEE Trans. Biomed. Eng.*, BME-21: 494-495, 1974.

[65] Klinger, "Heat Transfer in Perfused Biological Tissue – I: General Theory," *Bull. Math. Biol.*, 36: 403-415, 1974.

[66] H.C. Bazett, and B. McGlone, "Temperature Gradients in the Tissue in Man," *Am. J. Physiol.*, 82: 415-, 1927.

[67] J.W. Valvano, S. Nho, and G.T. Anderson, "Analysis of the Weinbaum-Jiji Model of Blood Flow in the Canine Kidney Cortex for Self-heated Thermistors," *ASME J. Biomech.*, 116: 201-207, 1994.

[68] H. Brinck, and J. Werner, "Estimation of the Thermal Effect of Blood Flow in a Branching Countercurrent Network Using a Three-Dimensional Vascular Model," *Trans. ASME,* 116: 324 - 330, 1994.

[69] Anderson, G.T., Valvano, J.W., 1989, "An Interlobular Artery and Vein Based Model for Self-Heated Thermistor Measurements of Perfusion in the Canine Kidney Cortex", ASME Winter Annual Meeting, *Bioheat Transfer - Applications in Hyperthermia, Emerging Horizons in Instrumentation and Modeling*. Roemer, McGrath and Bowman ed., HTD Vol. 126, BED Vol. 12, pp. 29-35.

[70] G.T. Anderson, and J.W. Valvano, “A Small Artery Heat Transfer Model for Self-Heated Thermistor Measurements of Perfusion in the Canine Kidney Cortex”, *J. Biomech Eng*, 116: 71-78, 1994.

[71] D.Y. Yuan, L.X. Xu, L. Zhu, K.R. Holmes, J.W. Valvano, Perfusion and Temperature Measurements in Hyperthermic Canine Prostates, 17th Southern Biomedical Engineering Conference, pg. 85, Feb 7-8, 1998.

[72] L.X. Xu, L. Zhu, K.R. Holmes, Thermoregulation in canine prostate during transurethral microwave hyperthermia, part II: blood flow response, International Journal of Hyperthermia. 14(1):65-73, 1998 Jan-Feb.